

Adaptive control schemes for engine sound quality improvement

L.P.R. de Oliveira*, B. Stallaert*, W. Desmet*, P. Sas*, K. Janssens†, H. Van der Auweraer†

* K.U.Leuven, Department Mechanical Engineering
Celestijnenlaan 300 B, B-3001, Leuven - Belgium

† LMS International
Interleuvenlaan 68, B-3001, Leuven - Belgium
email: leopoldo.deoliveira@mech.kuleuven.be

Abstract

Active noise control systems tend to be designed with a target on sound pressure level reduction. However, the perceived control efficiency for the occupants can be more accurately assessed if psychoacoustic metrics are taken into account. The aim of this paper is to evaluate the effect of an adaptive structural acoustic controller on the sound quality of engine noise in a vehicle mockup. The engine excitation is provided by a sound quality equivalent engine simulator, running on a real-time platform that delivers harmonic excitation in function of the driving condition. The controller targets a certain order to match a predefined profile. The controller performance is evaluated in terms of the tracked order amplitude and Zwicker Loudness.

1 Introduction

The successful development of new products relies on the capability of assessing the performance of conceptual design alternatives in an early design phase. In recent years, major progress was made hereto, based on the extensive use of virtual prototyping, particularly in the automotive industry. The novelty in this framework is to account for the human perception when defining product performance criteria [1,2].

Additionally, active control has shown the potential to enhance system dynamic performance which allows lighter and improved products. Research done in the last years on smart materials and control concepts has led to practical applications with promising results for the automotive industry [3]. However, to make the step to the design of active sound quality control (ASQC), the control schemes, along with appropriate simulation procedures, need to become an integral part of the product development process [4,5]. In other words, this requires: (i) the product performance metrics to be based on human perception attributes and (ii) the simulation models to support the specific aspects related to smart structures (active systems, actuators, sensors and control logic).

In order to demonstrate the proposed simulation procedure and evaluate the effect of active control on the perceived sound quality (SQ), a vibro-acoustic cabin mock-up is selected (Fig. 1). It consists of a simplified car cavity with rigid acoustic boundary conditions. The passenger compartment (PC) and the engine compartment (EC) are connected through a flexible firewall which allows noise generated in the EC to be transmitted to the PC. A sound source placed in the EC works as a primary disturbance source. The primary source is driven by a real-time engine simulator, capable of delivering a harmonic excitation based on the engine orders' amplitude and phase [6].

An adaptive feedforward controller with a structural secondary actuator and an acoustic error sensor is proposed. The control strategy results from a modified version of the Fx-LMS [7] to which modifications are proposed in order to improve the convergence rate. This control strategy is described in Section 2. In Section 3, the modeling procedure and simulation results are presented. The experimental validation and

the results obtained with such controller in terms of order profiles, Specific-Loudness and Zwicker-Loudness [8,9] are treated in Section 4. Finally, some general conclusions are addressed in Section 5.

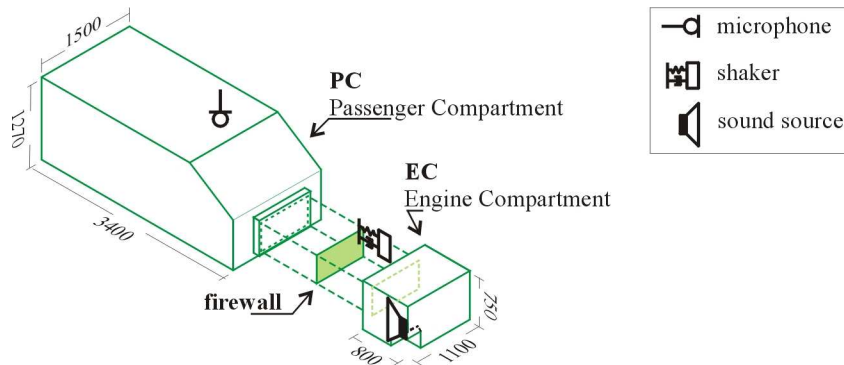


Figure 1 – Vehicle mock-up

2 Control Strategy

The aim of the proposed control scheme is to achieve a pre-defined order amplitude vs. RPM profile, not only for constant, but also for varying engine speeds. In this way, the controller has to be capable of tracking changes on the disturbance and converge, fast enough, to the desired output value, eventually resulting in the desired order balance.

Therefore, an adaptive feedforward strategy is proposed, which is a modified version of the standard Fx-LMS algorithm. The first modification aims at improving the convergence speed of the adaptive scheme, in order to cope with changing RPMs during normal engine operation. Eventually, equalization capabilities are implemented to allow the tuning of order amplitudes according to the RPM, thus achieving the desired sound quality target in an authentic Active Sound Quality Control (ASQC) fashion.

The improvement in convergence speed of the standard Fx-LMS [11] is achieved, initially, by compensating for the secondary path dynamics. Figure 2(a) and (b) show the standard and modified Fx-LMS block diagrams, respectively. In the latter, the gradient descent method can be seen as a standard LMS algorithm on \hat{x} and $(e + \hat{y})$, thus with convergence rate comparable with standard LMS schemes [7]. The error signal used in the modified version is an estimate of the primary disturbance signal d , in this way, diminishing the effect of the secondary path dynamics.

In addition to the modified Fx-LMS proposed by [7], a normalization of the reference signal is performed such that the convergence is optimized without destabilizing the controller. The maximum step size, μ , that leads to the fastest convergence without destabilizing the controller is given by Eq.(1), where L is the length of the FIR filter and P_x is the power of the reference signal x .

$$\mu < \frac{2}{LP_x} \quad (1)$$

This inequality is used to determine a variable step size in what is known as the normalized LMS (NLMS) algorithm [11]. In contrast with the NLMS, in this implementation, the normalization is obtained by filtering the reference signal through N such that, for a fixed step size, the reference signal power P_x is optimized for convergence (Fig. 2c).

Eventually, giving a fast converging adaptive scheme, an equalization capability is provided by the gain β (Fig. 2c), as suggested by [4]. However, in contrast with [4], the equalization is applied just before the secondary path and only there it is necessary, since the adaptive scheme is based on an estimation of d . As

a result of the equalization, the error signal is given by Eq.(2), where, given enough time to converge, $y(n)$ should tend to $d(n)$, which yields the approximation in Eq.(3).

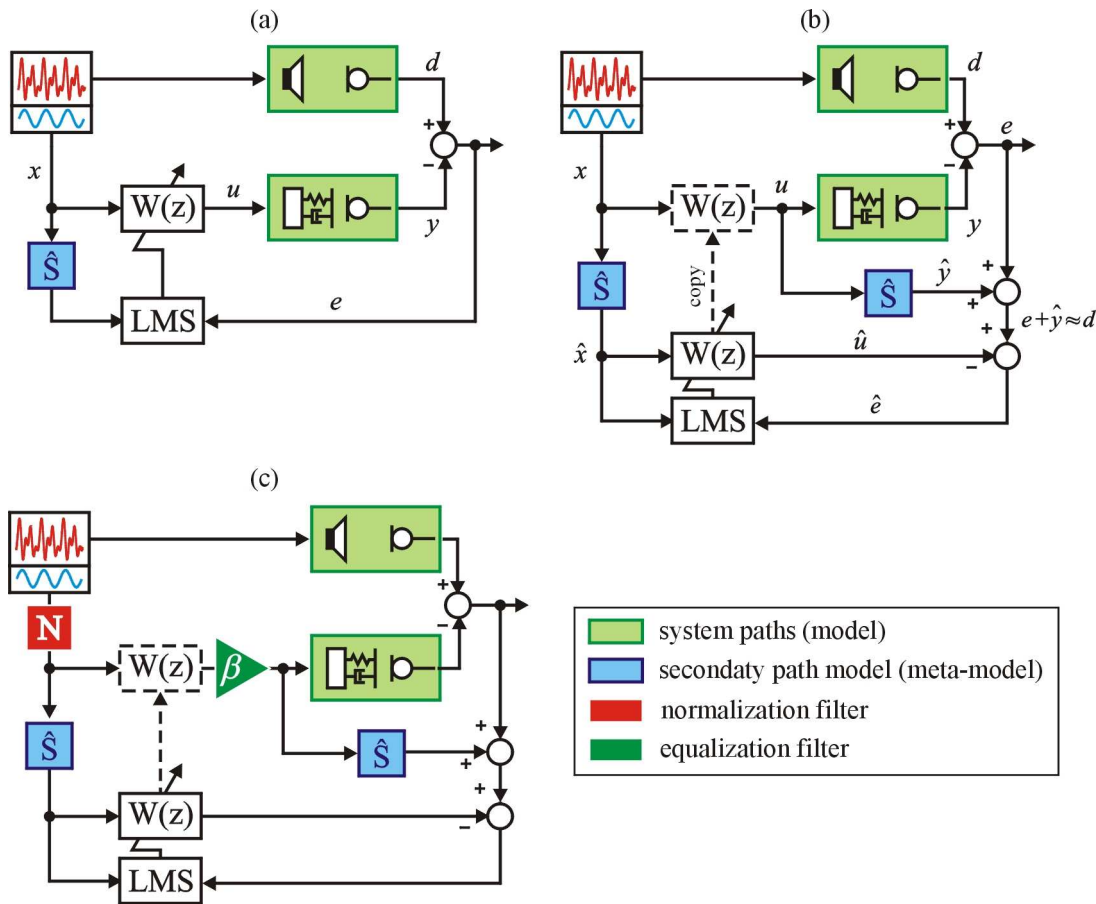


Figure 2 – Adaptive feedforward control schemes: (a) Fx-LMS, (b) modified Fx-LMS and (c) NEX-LMS

$$e(n) = d(n) - \beta y(n) \tag{2}$$

$$e(n) \approx (1 - \beta)d(n) \tag{3}$$

Equation (3) shows that the actual system output amplitude can be controlled by adjusting the gain value β . The system behaves symmetrically w.r.t. $\beta = 1$ the system will reduce the order amplitude as much as possible. Within the interval $0 < \beta < 1$, the system presents a residual error which is in between the passive order amplitude ($\beta = 0$) and minimum order amplitude ($\beta = 1$). The same holds for $1 < \beta < 2$, although with opposite phase. Outside these ranges, *i.e.*, $\beta < 0$ or $\beta > 2$ the system amplifies the original order amplitude.

Therefore, the proposed control scheme, hereafter referred to as NEX-LMS, features a fast converging adaptive algorithm based on the normalization of the reference signal and equalization capabilities, elements necessary for an engine sound quality controller.

3 System Modeling and Simulation Results

The modeling procedure presented here is a general framework in which different control strategies can be implemented, revealing the functionality of such an approach to the assessment of conceptual design performance [1,5,11].

One of the key aspects in this modeling approach resides in deriving reasonably sized models that integrate the structural and acoustic components along with the control algorithm. In order to fulfill this requirement, a fully coupled finite element (FE) model of the vibro-acoustic system is written as a modal state-space (SS) model (Eqs. 4 and 5). As a result of using the coupled vibro-acoustic modal base, any combination of structural and acoustic inputs/outputs can be used for the control design, e.g., an acoustic source in the EC, structural sensors and actuators on the firewall and microphones on the PC.

$$\begin{Bmatrix} \dot{\mathbf{q}} \\ \ddot{\mathbf{q}} \end{Bmatrix} = \begin{bmatrix} \mathbf{0} & \mathbf{I} \\ -\mathbf{\Omega}^2 & -\mathbf{\Gamma} \end{bmatrix} \begin{Bmatrix} \mathbf{q} \\ \dot{\mathbf{q}} \end{Bmatrix} + \begin{bmatrix} \mathbf{0} \\ \mathbf{\Phi}_L^T \mathbf{B} \end{bmatrix} \begin{Bmatrix} \mathbf{F}_s \\ \mathbf{F}_a \end{Bmatrix} \quad (4)$$

$$\begin{Bmatrix} \mathbf{u} \\ \mathbf{p} \end{Bmatrix} = \begin{bmatrix} \mathbf{C} \mathbf{\Phi}_R & \mathbf{0} \end{bmatrix} \begin{Bmatrix} \mathbf{q} \\ \dot{\mathbf{q}} \end{Bmatrix} \quad (5)$$

where \mathbf{q} is the vector of modal amplitudes of the Eulerian vibro-acoustic model in displacement \mathbf{u} and pressure \mathbf{p} ; \mathbf{B} and \mathbf{C} are Boolean matrices that select input and output DoFs, respectively; \mathbf{F} is the load vector, $\mathbf{\Phi}_L$ and $\mathbf{\Phi}_R$ are the left and right-eigenvector which hold the following properties:

$$\mathbf{\Phi}_L^T \begin{bmatrix} \mathbf{M}_s & \mathbf{0} \\ \rho_o \mathbf{K}_c^T & \mathbf{M}_a \end{bmatrix} \mathbf{\Phi}_R = \mathbf{I} \quad (6)$$

$$\mathbf{\Phi}_L^T \begin{bmatrix} \mathbf{K}_s & \rho \mathbf{K}_c \\ \mathbf{0} & \mathbf{K}_a \end{bmatrix} \mathbf{\Phi}_R = \mathbf{\Omega}^2 \quad (7)$$

$$\mathbf{\Phi}_L^T \begin{bmatrix} \mathbf{D}_s & \mathbf{0} \\ \mathbf{0} & \mathbf{D}_a \end{bmatrix} \mathbf{\Phi}_R = \mathbf{\Gamma} \quad (8)$$

where ρ_o is the air density, the index a refers to acoustic and s to structural DoFs, \mathbf{K} , \mathbf{D} and \mathbf{M} are the stiffness, damping and mass matrices, respectively, and \mathbf{K}_c is the vibro-acoustic coupling matrix; \mathbf{I} is the identity matrix, $\mathbf{\Omega}$ is the matrix of natural frequencies and $\mathbf{\Gamma}$ is the modal damping matrix. For a more detailed description of the state-space model, the reader is referred to [10].

The original FE model, consisting of the firewall and the cavities, contains 24192 DoFs (23196 unconstrained acoustic and 1026 unconstrained structural). Applying the aforementioned modal reduction, it has been reduced to a SS model with $2 \times N$ DoFs, related to the N kept modes, with force and volume velocity as inputs and displacement and pressure as outputs. The modal base was built with modes ranging from 0 to 400Hz, resulting in $N = 107$.

For the adaptive feedforward simulations, a meta-model is needed to represent $\hat{\mathbf{s}}$ as a FIR filter. As depicted in Fig. 3, this meta-model can be obtained with an LMS-based off-line estimation [11], where measurement noise is represented by $\nu(n)$. After convergence, the FIR filter $\mathbf{W}(\mathbf{z})$ resembles the secondary path transfer function in a completely analogous way as during the practical implementation. Eventually, the block diagram for simulating the adaptive control scheme can be used as in Fig. 4.

In this implementation, the reference signal is a sine wave of constant amplitude and the same frequency as the targeted order. In this fashion, the control system should behave as an adaptive notch-filter [11], with minimum (or none) effect on the other orders. The frequency sample used is 2kHz. The length of the FIR filter $\hat{\mathbf{s}}$ is 2000, while \mathbf{W} is 10. For stationary RPMs, the whole of filter \mathbf{N} is that of a gain, which keeps the amplitude of the filtered reference signal as high as possible, so as to achieve convergence as fast as possible without destabilizing the system.

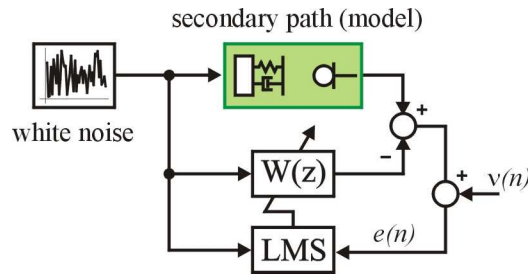


Figure 3 – Block diagram of the secondary path offline identification

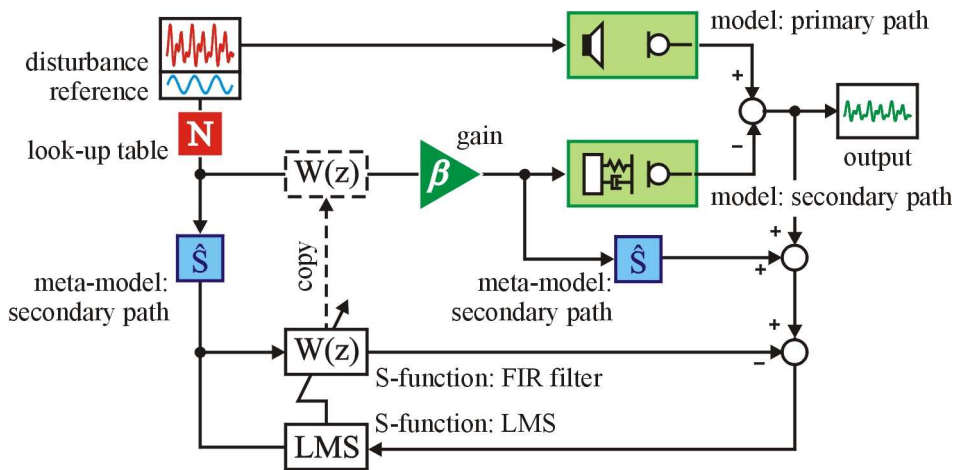


Figure 4 – Block diagrams for the NEX-LMS simulation

In order to have an engine-like excitation, which allows meaningful SQ measurements, a real-time engine simulator was used [6]. A real-time engine simulator provides a SQ-equivalent disturbance in function of speed, gear and load and allow the engine to be virtually driven. This platform can be used for both, simulation and measurements. The order cuts used here are depicted in Fig. 5 and correspond to 50km/h (1634rpm) and 80km/h (2694rpm) driving conditions. The excitation consists of 20 complex orders (0.5, 1.0, 1.5, ..., 10). Due to the SQ equivalence of the excitation, SQ metrics can be calculated from the resulting pressure signals, from which rather general conclusions can be drawn.

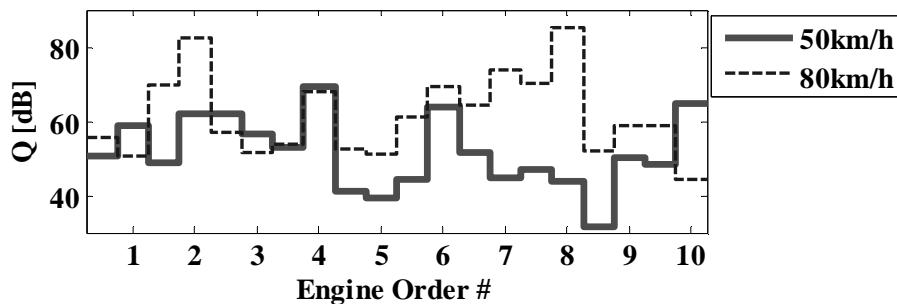


Figure 5 – Order amplitudes for two driving conditions

The passive and active order profiles for the microphone placed at the driver’s head position are depicted in Fig. 6. The simulated results indicate that the controller indeed behaves like a notch filter, affecting only the desired order, which is an important feature towards Active Sound Quality Control. These results also suggest that such controllers can be added in parallel without cross-talk between them.

The effect of the control action on the engine sound quality can be seen in Fig. 7. The selected SQ metric is Zwicker Loudness, which is linearly related to the human perception of volume [8,9]. The Specific Loudness contours for the system with and without control can be seen in Fig. 7 for both driving conditions: 50km/h and 80km/h. In the former, most of the noise is due to the presence of the 2nd order, which when controller, reduces significantly the overall Zwicker Loudness (Tab.1). At 80km/h, the effect of the controller is greater in the 0~2Bark range, as only the 2nd order is controller, higher critical bands are not affected.

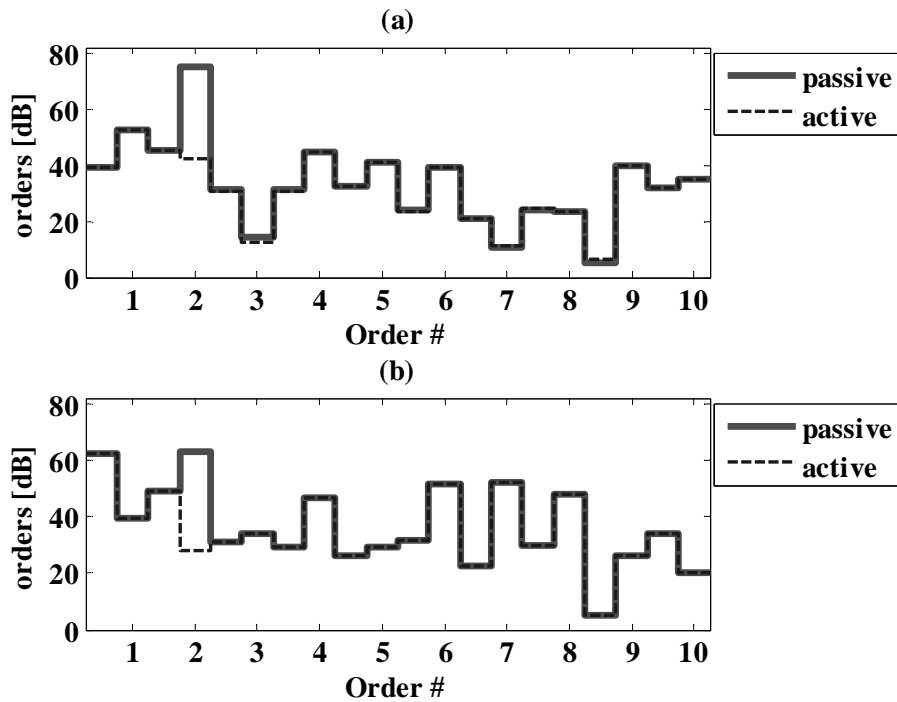


Figure 6 – Passive and active order amplitudes for (a) 50km/h and (b) 80km/h

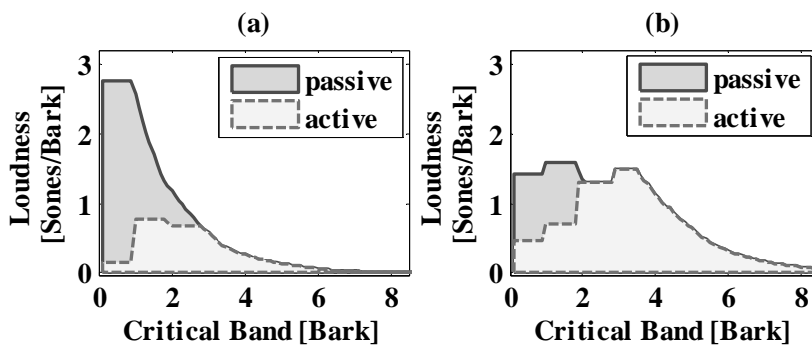


Figure 7 – Specific Loudness (a) @ 50km/h and (b) @ 80km/h

Table 1 - Zwicker Loudness [Sones]

	50km/h	80km/h
passive	6.1	7.5
active	2.4	5.8

In the next section, the numerical validity of the reduced model is illustrated by comparing FRFs from the original FE model with the reduced SS model and measured FRFs against the identified secondary path FIR filters. Also, the same engine excitation is applied to the vehicle mock-up and the results are compared to simulations.

4 Experimental Validation

Figure 8 shows the experimental setup. The structural excitation is performed with a LDS shaker (model V201/3), the force transducer is a PCB 208C04 and the accelerometers are PCB 352C67. Fig. 8(b) shows the acoustic source (LMS E-LMFVVS) placed at the EC. The microphones used are B&K 4188. For the system validation, either the shaker or the acoustic source were fed with white noise. The FRFs are measured with an Hv estimator, while input and output signals are filtered with Hanning windows. The controller is implemented in a modular 1006 dSpace system.

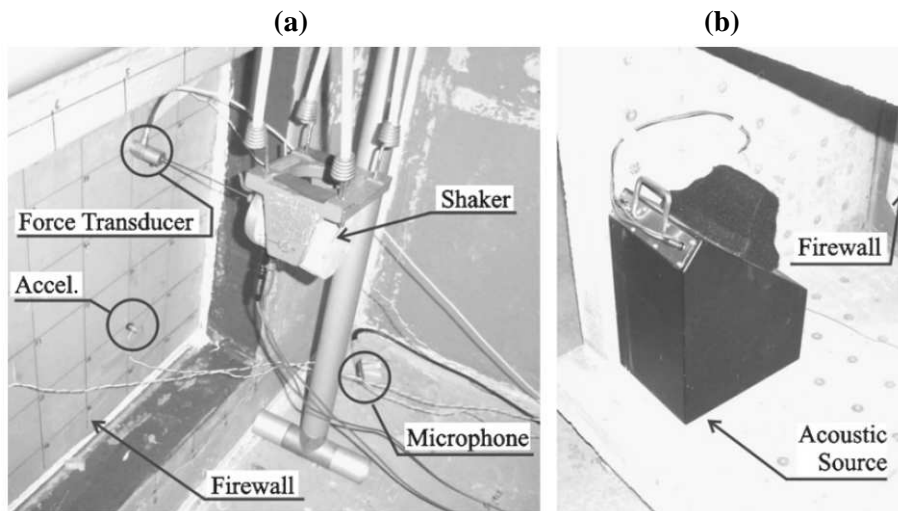


Figure 8 – Experimental setup: (a) shaker and sensors attached to the firewall and (b) sound source in the engine compartment

In Figure 9, the FRFs derived from the reduced SS model are compared with the FRFs measured on the cabin mock-up. The system inputs are volume velocity applied in the EC (acoustic input) and force applied on the firewall (structural input); and the outputs are pressure measured in the PC (acoustic output) and displacement measured on the firewall (structural output). These FRFs include the transfer paths to the driver's microphone from both inputs: primary acoustic source and secondary structural actuator. The vibro-acoustic system has been excited with white noise. The FRFs are measured with an Hv estimator, while input and output signals are filtered with Hanning windows. The good correlation between the SS and the FE model validates the model reduction procedure.

For the adaptive controller, the reference for the FRFs should be the voltage signal sent to either the shaker (V_s) or the acoustic source (V_p) as in Fig. 10. A comparison of such FRFs and the magnitude of the identified FIR filters in the frequency domain is presented. For the practical implementation of the adaptive feedforward control, the FIR filter \hat{S} is estimated as depicted in Fig. 3. The frequency sample for the real-time DSP is 2kHz. The frequency of 10th order at 80km/h is 450Hz, well below the DSP Nyquist frequency.

In both cases (Figs. 9 and 10) the comparisons present a good agreement. Few discrepancies arise, a.o., from the lack of accuracy in determining the exact place of the disturbance source, sensor/actuator pair and microphones and from assuming the disturbance source as an ideal point source. Such mismatches are expected and believed not to harm the accuracy of the results, as previous analyses have shown [1,5,10].

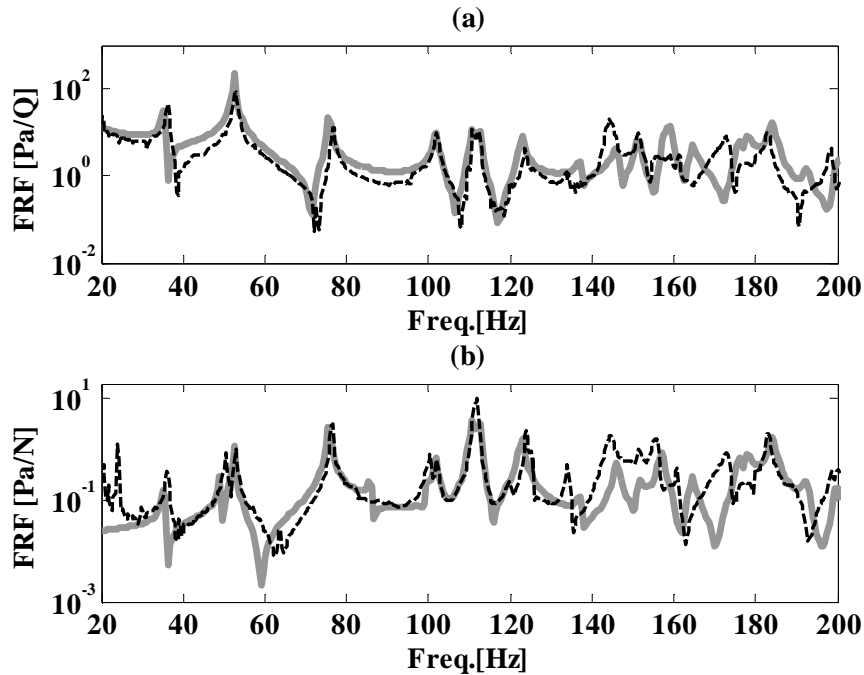


Figure 9 – Comparison of (---) experimental and (—) numerical FRFs:
(a) acoustic input and (b) structural input

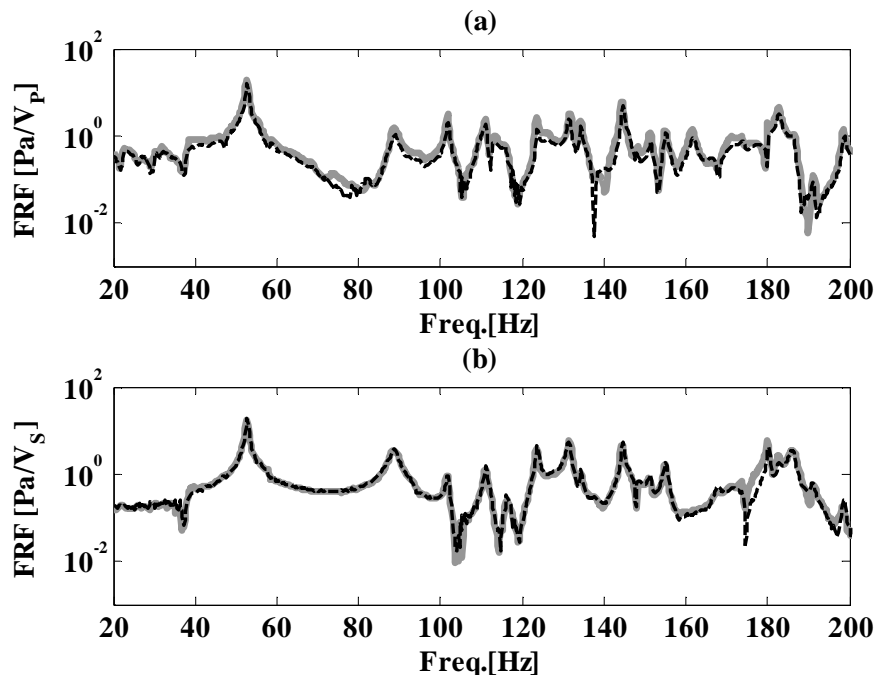


Figure 10 – Comparison of (---) FRFs and (—) FFT of identified FIR filters:
(a) primary and (b) secondary paths

As mentioned before, a real-time engine simulator was used to excite the system. SQ-equivalent engine models are used in product development, as it enables one to experience and assess the NVH of a virtual (or real) vehicle under various driving conditions [6,12]. The novelty here is the use of such device as a source of excitation. In this case, the engine sound, which is a function of the driving condition (engine speed, gear, throttle and brake positions, etc.) is fed to the acoustic source in the EC. Results obtained as such, benefit from this SQ-equivalence and, therefore, allow the correlation with real engine sounds.

Figure 11 shows the experimental order amplitudes measured by the driver’s microphone with controller on and off for both driving conditions. The 2nd order is targeted in both cases and the reduction obtained specifically for this order is 34dB for 50km/h and 51dB for 80km/h.

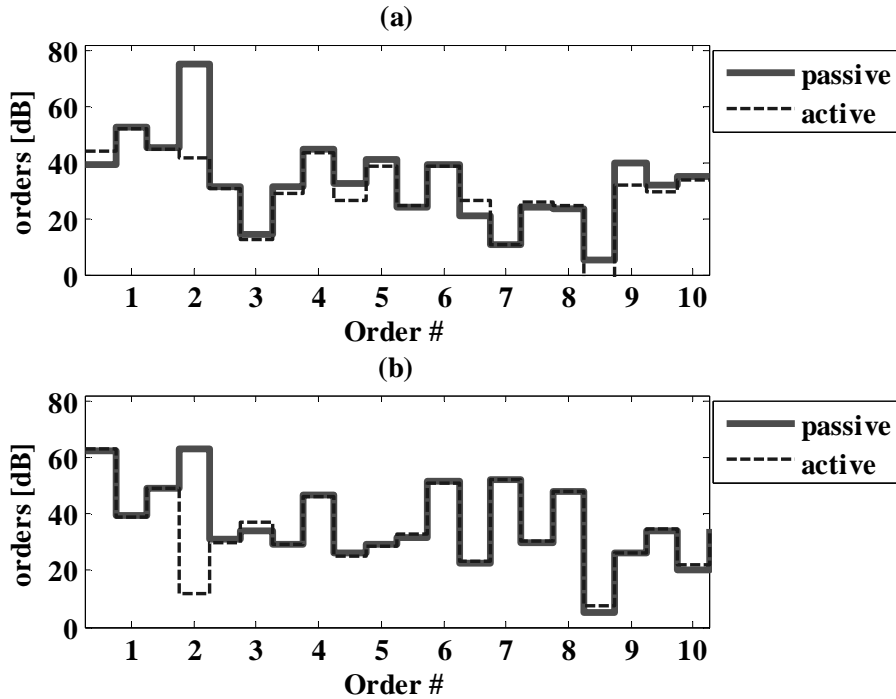


Figure 11 – Order amplitudes for feedforward control and two driving conditions, (a) 50km/h and (b) 80 km/h

The Specific Loudness plots for 50km/h and 80km/h are shown in Fig.12. In agreement with the simulated predictions, even if the controller is targeting just a single order, the effect on the perceived loudness is quite noticeable. The Specific Loudness contours, as well as the Zwicker Loudness values (Table 2) for passive and active systems show a good agreement with the simulated data and reveal the efficiency of such control approach.

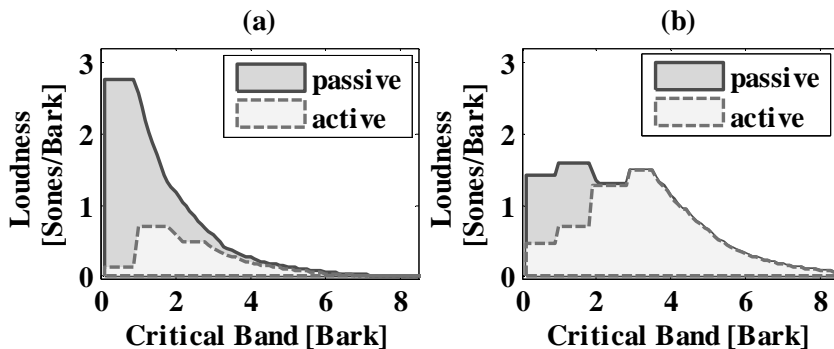


Figure 12 – Specific Loudness (a) @ 50km/h and (b) @ 80km/h

Table 2 - Zwicker Loudness [Sones]

	50km/h	80km/h
passive	6.1	7.5
active	1.9	5.8

Figure 13 shows the controller performance in time-domain, i.e., its capability of converging to the desired amplitude when a new RPM is presented. This feature is illustrated by comparing the 2nd order cuts for the modified Fx-LMS and the proposed NEX-LMS scheme. These simulation results show that the NEX-LMS outperform the modified Fx-LMS which was already proposed as a faster alternative to the standard Fx-LMS [7]. After 500 iterations (.25s @ 2kHz frequency sample) the NEX-LMS has reduced 40dB while the modified algorithm 7dB.

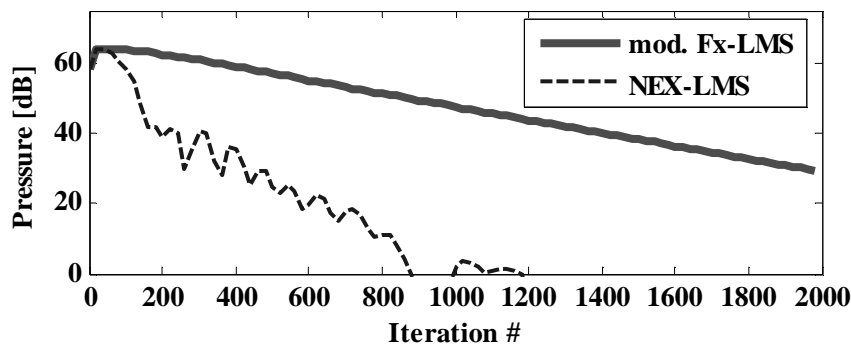


Figure 13 – 2nd order cuts for (—) modified Fx-LMS and (---) NEX-LMS.

5 Conclusions and Future Work

This paper describes a modeling procedure for ASAC, which allows the use of standard vibro-acoustic FE models in the control design. The modeling procedure is experimentally validated with a vehicle mock-up.

The proposed experimental setup is acoustically excited by a SQ-equivalent engine simulator, typically employed in auralization. The use of such scheme allows repeatable measurements with engine-like excitation signals, furnishing results that can be directly correlated to automotive applications.

The results for Loudness attenuation are presented in terms of Specific and Zwicker Loudness, the latter being linearly related to the human sensation of volume. The results indicate that the controller is quite effective with respect to the occupants' perception of the sound field. Also, it was possible to control an order independently from the others, which is an interesting feature for the intended future application of such controllers, i.e., order balancing. In order to independently tune multiple orders, similar controllers could be connected in parallel since each narrowband action would not interfere with each other.

The improved convergence speed of the presented adaptive feedforward control indicates it could cope with varying engine speed.

A next step in this study is to investigate the effect of such a controller in the whole cavity and extend the SQ investigation to Roughness. The only way to improve Roughness is through order balancing, which this scheme is capable of. The desired order profiles (amplitude and phase vs. RPM) can be defined with the aid of SQ-equivalent models and further used to define target values for the feedforward controller.

Acknowledgements

The research of Leopoldo P. R. de Oliveira is supported in the framework of a bilateral agreement between the Katholieke Universiteit Leuven in Belgium and the University of São Paulo in Brazil. The research presented in this paper was performed as part of the Marie Curie RTN project: A Computer Aided Engineering Approach for Smart Structures Design (MC-RTN-2006-035559).

References

- [1] L.P.R. de Oliveira, *et al.*, Active sound quality control of engine induced cavity noise, *Mechanical Systems and Signal Processing* (2008), doi:10.1016/j.ymssp. 2008.04.005
- [2] D. Berckmans, *et al.*, Model based synthesis of aircraft noise to quantify human perception of sound quality and annoyance, *Journal of Sound and Vibration* 311 (2008) 1175-1195.
- [3] S. Hurlebaus, L. Gaul, Smart structure dynamics, *Mechanical Systems and Signal Processing*, 20 (2006) 255-281.
- [4] S.M. Kuo, A. Gupta, S. Mallu, Development of adaptive algorithm for active sound quality control, *Journal of Sound and Vibration*, 299 (2007) 12-21.
- [5] H. Van der Auweraer, *et al.*, Virtual prototyping for sound quality design of automobiles, *Sound and Vibration*, April (2007) 26-30.
- [6] K. Janssens, P. Van de Ponsele, M. Adams, The integration of sound quality equivalent models in a real-time virtual car sound environment. *Proceedings of DAGA Conference*, 18-20 March, 2003, Aachen, Germany, 6p.
- [7] C. Bao, Adaptive algorithms for active noise control and their applications, PhD Thesis, Katholieke Universiteit Leuven, Mechanical Engineering Department – PMA, 1994.
- [8] E. Zwicker, H. Fastl, *Psychoacoustics: Facts and Models*, Springer Series in Information Sciences, Heidelberg, 1999, Ed.2.
- [9] International Organization for Standardization, *Method for Calculating Loudness Level*, ISO-532B, 1975.
- [10] L.P.R. de Oliveira, *et al.*, Concurrent mechatronic design approach for active control of cavity noise, *Journal of Sound and Vibration*, 314 (2008) 507–525
- [11] S.M Kuo, D.R. Morgan, *Active Noise Control Systems: Algorithms and DSP implementation*, John Wiley and Sons, Inc. – New York (1996).
- [12] R. Williams, *et al.*, Using an interactive NVH simulator to compute and understand customer opinions about vehicle sound quality, *Symposium on International Automotive Technology*, 2007, Pune, India, SAE Paper No. 2007-26-036.

